Experimental determination of preferred instability modes in a mechanically excited thermal plume by ultrasound scattering

J.C. Elicer-Cortés [a,*], A. Navia [a], D. Boyer [b], M. Pavageau [c], R.H. Hernández [a]

[a] *Departamento de Ingeniería Mecánica, Universidad de Chile, Beauchef 850, 5º Piso, Casilla 2777, Santiago, Chile*
[b] *Instituto de Física, Universidad Nacional Autónoma de México, Apartado Postal 20-364, 01000 México DF, Mexico*
[c] *Ecole des Mines de Nantes, GEPEA, UMR CNRS 6144, 4, rue Alfred Kastler, B.P. 20722, F-44307 Nantes Cedex 3, France*

Abstract

Ultrasound scattering is used to characterize instability modes in a laminar axisymmetric thermal plume subjected to controlled axisymmetric (''varicose'') disturbances. A scattered signal is detected as soon as vortical structures appear in the flow, whereas temperature inhomogeneities have almost no effects on scattering. In the absence of any disturbances, the flow remains laminar and quite stable, which was corroborated with Schlieren visualizations. Scattering peaks exhibited maxima around forcing frequencies of $f = 2$ Hz. By increasing the mechanical forcing frequency, the amplitude of the scattering peak decreases and disappears for higher forcing frequencies, revealing a relaminarization process. For frequencies around $f = 1$ Hz and lower, no scattering is observed, like without forcing. The study of the normalized amplitude of the scattering peak at different structure sizes enables the identification of two ranges of preferred wavelengths of instability modes: the first ranges from $l = 80$ mm to $l = 54$ mm and the second from $l = 20$ mm to $l = 16$ mm. These preferential space modes can be attributed to natural frequencies of the flow. The levels of vorticity of the preferential modes depend on the frequency of the mechanical disturbance, being maximum around $f = 2$ Hz. The position of the maximum of vorticity moves to higher values of frequency as the temperature is increased. When the mechanical forcing frequency increases away from the resonance frequency, vorticity decays gradually reaching very low values. High frequency disturbances do not destabilize the thermal plume, which acts as a filter.

Keywords: Thermal plume; Instability modes; Vorticity; Ultrasound scattering

1. Introduction

This paper focuses on the stability of a thermal plume, in which buoyancy forms the main source of fluid motion. The sensitivity of this type of flows to even slight disturbances (natural or imposed) is such that initially laminar regimes often become turbulent rather quickly.

The question of how and when buoyancy-driven flows become turbulent is an important matter from the applicative point of view. Cetegen et al. [1] illustrated the practical importance of studying fluid motion resulting from buoyancy-induced convection. The main point is that heat, mass or momentum transfer rates, among others, are rather different depending on whether a flow is laminar or turbulent. Thus, turbulence will generally be fostered any time high mixing efficiency is sought for. More interesting, perhaps, is that initially laminar flows may react differently to mechanical disturbances of different frequencies: a given disturbance may be damped or amplified so that turbulence may develop or not, at more or less fast rates. Consequently, a better knowledge of the preferential modes of a given flow may make it possible ultimately to design control systems able to trigger or inhibit the growth of turbulence depending on the targeted application. In other cases, it may merely be useful to be able to tune the pulsing, puffing or flapping frequency of a flow to a desired frequency,

* Corresponding author. Tel.: +56 2 978 45 42; fax: +56 2 698 84 53.
E-mail address: jelicer@cec.uchile.cl (J.C. Elicer-Cortés).

Nomenclature

Symbols

A	amplitude of scattering peak, V
A_{dB}	amplitude of scattering peak, dB
A_{FR}	amplitude of frequency response of transducers, V
$A_{\mathrm{FR\,dB}}$	amplitude of frequency response of transducers, dB
A_{n}	normalized amplitude of scattering peak
c	speed of sound, m/s
D	diameter of the disk heated source, m
e	2.71828...
f	mechanical forcing frequency, Hz
F	scattering Doppler shifting [$=(\nu - \nu_0)$], s^{-1}
$\vec{g}$	uniform gravitational field, $\mathrm{m/s}^2$
Gr	Grashof number ($=g\beta(T_{\mathrm{d}} - T_\infty)D^3/\eta^2$)
i	$\sqrt{-1}$
$\vec{k}$	wave vector, m^{-1}
$\vec{k}_{\mathrm{s}}$	scattering direction wave vector, m^{-1}
$\vec{k}_{\mathrm{i}}$	incoming direction wave vector, m^{-1}
l	characteristic length scale of flow, m
P_0	pressure amplitude of the incoming sound wave, Pa
$\tilde{p}_{\mathrm{scat}}$	total scattering pressure Fourier transform in space and time, Pa m^3 s
$\tilde{p}_{\mathrm{scat}}^{\mathrm{temp}}$	scattering pressure Fourier transform in space and time due to temperature fluctuations, Pa m^3 s
$\tilde{p}_{\mathrm{scat}}^{\mathrm{vort}}$	scattering pressure Fourier transform in space and time due to vorticity, Pa m^3 s
$\vec{q}$	wave vector, m^{-1}
q	magnitude of wave vector, m^{-1}
r	transverse cylindrical coordinate, m
Ri	Richardson number of a free jet ($=[(\rho_\infty - \rho_{\mathrm{j}})gw]/\rho_\infty U_{\mathrm{j}}^2$)
St	Strouhal number ($=fD/U_{\mathrm{a}}$)
t	time, s
$\tilde{T}$	Fourier transform in space and time of temperature fluctuations, K m^3 s
T_{d}	temperature of the heated disk, K
T_0	flow mean temperature, K
T_∞	quiescent medium fluid temperature, K
U_{a}	mean advection velocity of vortical structures, m/s
U_{j}	mean velocity of a free jet at nozzle exit, m/s
$\vec{V}_{\mathrm{inc}}$	velocity field of incident sound wave, m/s
$\vec{V}_0$	velocity field amplitude of incident sound wave, m/s
$\vec{x}$	position vector of receiver transducer with respect to measurement volume, m
w	slot width of a bidimensional jet, m
z	axial cylindrical coordinate, m

Greek symbols

β	volumetric coefficient of thermal expansion, K^{-1}
δ	differential operator of a variable
$\Delta\nu$	scattering Doppler shifting [$=(\nu - \nu_0)$], s^{-1}
θ	scattering angle, rad
η	kinematic viscosity, m^2/s
ν	scattered sound wave frequency, s^{-1}
ν_0	incoming sound wave frequency, s^{-1}
λ	wavelength scale of acoustic field, m
π	3.14159...
ρ	fluid density of flow interacting with sound, $\mathrm{kg/m}^3$
ρ_{j}	density of the fluid flow of a free jet, $\mathrm{kg/m}^3$
ρ_0	mean fluid density of flow without interaction, $\mathrm{kg/m}^3$
ρ_∞	fluid density at ambient temperature, $\mathrm{kg/m}^3$
$\vec{\omega}$	vorticity, s^{-1}
$\tilde{\vec{\omega}}$	Fourier transform in space and time of vorticity, m^3

or to look for the development of structures of specified scales. For example, in an axisymmetric plume rising from a flame, the periodic engulfment of air produced by the large-scale toroidal vortex rings forming close to the source is responsible for most of the plume entrainment. These vortices generate a periodic pumping whose magnitude is directly related to their circulation [2]. The model derived by Cetegen subsequently to his analysis provided a sounder foundation for the scaling of entrainment rates in the near field of fire plumes, which is of great interest with respect to fire safety science and engineering even though incidental fires are not controllable flows.

The fate of a given disturbance in a given flow is not an easy matter. Basically, a disturbance evolves according to the net amount of energy input into it as it progresses downstream. The unstable behavior of a flow can be local or global, depending on whether a disturbance, initially located in space and time, will invade the whole flow or remain confined in a finite volume while it is simultaneously transported by the mean flow. Thus, the behavior of a disturbance depends on the intimate structure of the considered flow and, incidentally, of its environment.

Stability loss in thermal plumes pertains to a broader class of problems namely stability analysis of open systems (jets, wakes). The primary mechanism that makes initially laminar flows to become turbulent is the initial growth of very small disturbances. The study of these instabilities has been approached commonly by means of linear analysis. The approach consists in considering the effect of small departures from the equilibrium state by imposing velocity and/or temperature usually periodic disturbances much smaller than the velocity and/or temperature spatial varia-

tions within the developing laminar flow. Subsequently, only first-order, or linear, terms in the disturbance quantities are retained in the disturbed transport equations. This approximation along with others leads to considerable simplifications in the problem analysis. The approach has been explained in a rather clear way by Gebhart et al. [3]. From this, it has been found that a frequent mechanism of disturbance growth in buoyancy-induced flows is a propagating downstream periodic wave alike the Tollmien–Schlichting wave observed in forced boundary layer flows. If the flow and buoyancy forces are able to continuously supply energy to these waves, the disturbance will grow in amplitude. Now, the process is selective so that the amplification or damping of a periodic wave depends on its frequency. Moreover, it is location dependent. The fate of a wave at a given frequency can be examined through so-called stability planes (see [3]). Generally speaking, it has been observed that disturbances grow more quickly in free-boundary flows like heated plumes. The explanation is presumably the absence of solid surfaces to damp disturbances. Finally, when the amplitude of disturbances grows beyond the validity domain of the small disturbance approximation, non-linear growth mechanisms appear that generate higher harmonics and secondary flows. Thus, the transition from laminar to turbulence is governed initially by linear mechanisms while non-linear effects prevail later.

Several studies have allowed establishing certain characteristics of instability phenomena for two-dimensional flows. Pera and Gebhart [4] introduced small symmetric and asymmetric perturbations in two-dimensional heated air plumes. They observed that high frequency disturbances did not affect the stability of the studied plumes. In a plane plume, Bill and Gebhart [5] observed that transition to turbulence occurred simultaneously for both the temperature and velocity fields. Temperature and velocity disturbances were permanently coupled with each other. Disturbances were amplified in a selective fashion (frequency response of flow). After the boundary layer had broken, the fluid adapted to the turbulent characteristics and non-linear effects started to become predominant.

It is interesting to note that the wavelength or the frequency of the waves developing in a plume (or in a jet) is usually well correlated with the characteristic dimensions of the studied flow or with the characteristics of the disturbance source. Thus, in a theoretical and experimental work on an axisymmetric plume, Kimura and Bejan [6] noticed that during transition, the wavelength of the developing undulations at the plume boundary was well correlated to the local plume diameter. Cetegen [7] experimentally studied the effects of external disturbances on the behavior of axisymmetric helium and air–helium plumes. He observed that the immediate response of the plumes to imposed periodic disturbances was the regular formation of toroidal vortices at a frequency equal to the excitation frequency. These structures were then advected downstream by the mean flow. These large-scale structures had dimensions of the order of the source diameter. Additionally, the main flow field appeared not to be influenced by the mechanical forcing frequency as long as this frequency was not too close from the natural frequency of the flow. Similar experiments were performed by Cetegen et al. [1] for planar buoyant plumes of air–helium mixtures. It was investigated how the source width, the gaseous mixture exit velocity and the plume fluid density affected the formation of instabilities. The onset of pulsations within a height of a few nozzle widths from the source could be best correlated in terms of the plume source Reynolds number and the ratio of the initial mixture density to that of the ambient fluid. The oscillation frequency of the investigated plume configurations appeared to correlate well in terms of the Strouhal number $St = fw/U_0$ and the Richardson number Ri yielding a correlation $St = 0.55Ri^{0.45} (1 < Ri < 10^2)$. This correlation differs slightly from that obtained for axisymmetric buoyant plumes because of differences in the corresponding mixing rates and in the strength of the local buoyancy flux. Moreover, the vortex pairs developing at a planar plume boundary were found not as stable as the vortex rings observed in axisymmetric plumes.

In this paper, we present an experimental study of an initially laminar axisymmetric plume subjected to symmetric and periodically controlled disturbances (varicose mode). In the present case, measurements were performed by using a non-intrusive technique based on ultrasound scattering. Although the technique is well adapted to the analysis of flow instabilities [8–14], it seems that it was never applied to the stability analysis of perturbed laminar round thermal plumes. It however holds several advantages over alternative techniques: it allows a selective tracking of temperature and/or vorticity scales; the technique makes it possible to determine the advection velocity of these scales without invoking Taylor's hypothesis; various flow statistics within a finite volume can be obtained in a short time; it provides a way of decomposing the flow into space modes, i.e., it sorts out the unstable modes or the vortices according to their relevant frequency or size, respectively.

We have investigated several configurations by varying the source temperature (in a range where it did not influence the measurement of vorticity by the ultrasound technique), as well as the excitation frequency of the mechanical disturbance imposed on the flow. In the following, the main aspects of the technique are briefly recalled. We then describe the experimental apparatus utilized. This is followed by the presentation of the results and discussion of the preferred instability modes. We conclude this paper with a summary of the findings of this study.

2. Measurement technique

Numbers of theoretical and experimental studies [8–20] have developed and applied ultrasound scattering as a non-intrusive measurement technique for unstable flows. The technique consists in emitting an acoustic wave towards a volume of fluid in motion. When the wavelength

(λ) of the incoming acoustic wave is of the order of a characteristic length scale (l) of the flow under study, the acoustic mode may couple to the flow modes of vorticity and/or entropy (temperature), generating scattered waves. Based on the analysis of Chu and Kovásznay [18], Lund and Rojas [21] and Contreras and Lund [22] showed that, in a first Born approximation, the scattered acoustic pressure can be decomposed in two parts, $\tilde{p}_{\text{scat}} = \tilde{p}^{\text{vort}}_{\text{scat}} + \tilde{p}^{\text{temp}}_{\text{scat}}$, that are proportional to the Fourier transform in space and time of the vorticity $\tilde{\vec{\omega}}(\vec{q}, \nu - \nu_0)$ and of the temperature fluctuations $\widetilde{T}(\vec{q}, \nu - \nu_0)$, respectively. The wave vector $\vec{q} = \vec{k}_s - \vec{k}_i = (2\pi/c)(\nu\hat{x} - \nu_0\hat{s})$ is shown in Fig. 1, for a typical experimental set-up, where a second acoustic transducer is used to detect the scattered signal. The contributions to the scattering pressure read [22].

$$\tilde{p}^{\text{vort}}_{\text{scat}}(\vec{x}, \nu) = \frac{i\rho_0\pi^2\nu e^{i\frac{\nu|\vec{x}|}{c}}}{c|\vec{x}|}\left(\frac{-\cos\theta}{1-\cos\theta}\right)(\vec{V}_0 \wedge \hat{x}) \cdot \tilde{\vec{\omega}}(\vec{q}, \nu - \nu_0) \quad (1)$$

$$\tilde{p}^{\text{temp}}_{\text{scat}}(\vec{x}, \nu) = \frac{\rho_0|\vec{V}_0|\pi^2\nu^2 e^{i\frac{\nu|\vec{x}|}{c}}}{cT_0|\vec{x}|}\cos\theta\widetilde{T}(\vec{q}, \nu - \nu_0) \quad (2)$$

The derivation of Eqs. (1) and (2) relies on a few assumptions [21,22]: the flow Mach number is low, the thermal conductivity is constant and the ultrasound time scale is much shorter than flow time scales. As measurements are over a volume in real space (or "global"), the technique provides point measurements in Fourier space. A good spectral resolution will be obtained at the expense of the resolution in real space, and vice-versa. From Eqs. (1) and (2), the contributions to scattering by vorticity and by temperature fluctuations can be discriminated by appropriately choosing the relative orientation of the acoustic emitter and receiver. The scattered signal is composed of waves of frequencies (ν) close to the incoming ultrasound frequency ν_0. At low Mach numbers, $[(\nu - \nu_0)/\nu_0] \ll 1$, and the absolute value of the wave vector $\vec{q}$ simplifies to $|\vec{q}| \approx [4\pi\nu_0 \sin(\theta/2)]/c$. Subsequently, keeping the scattering angle θ constant for a given measurement height, the wave vector $\vec{q}$ solely depends on the incoming ultrasound frequency ν_0 and scans flow scales of characteristic length l given by: $|\vec{q}| \approx [4\pi\nu_0 \sin(\theta/2)]/c \approx (2\pi/l)$. It is therefore possible to study a particular flow length scale l by simply tuning the incoming sound wave frequency ν_0.

The expressions (1) and (2) were obtained in a first Born approximation, assuming that each elementary fraction of the measurement volume scatters the incident wave only once, multiple scattering events (producing lost of coherence) being negligible. A second approximation made is that of the far field limit, i.e., the characteristic length scale of the measurement volume is much smaller than its distance to the receiver transducer. Both assumptions are fulfilled in our experiment. As shown in Ref. [17,22] for instance, the first Born approximation is valid if the ultrasound wavelength is larger than the typical vortex core size multiplied by the Mach number. Since the Mach number is small here ($0.3/340 \approx 0.001$), even the smallest probe wavelength in this study is well above this limit.

In a typical ultrasound scattering experiment shown in Fig. 2(a), the scattered amplitude spectra (A_n) exhibits a

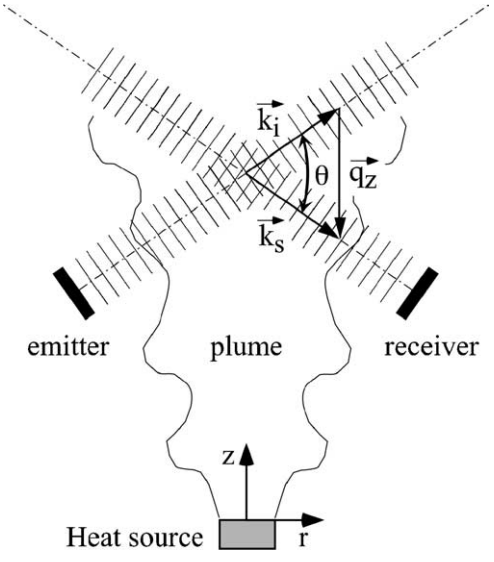

Fig. 1. Schematic representation of the non-intrusive coupling between the thermal plume and the ultrasound wave.

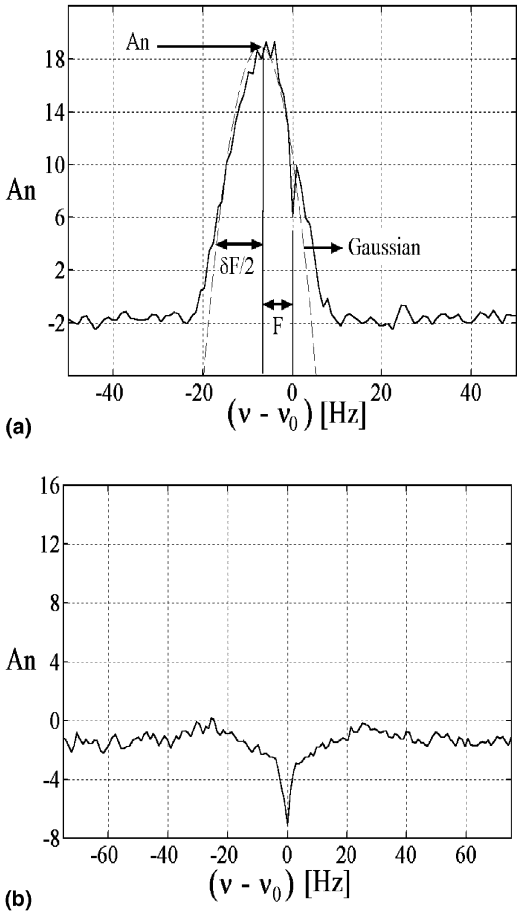

Fig. 2. Normalized amplitude of the scattering peak ($T_d = 150\,^{\circ}\text{C}$, $\nu_0 = 7.5$ kHz): (a) for disturbed condition, ($f = 2.5$ Hz); (b) for no disturbed condition, ($f = 0.0$ Hz).

frequency broadening (δF) related to the turbulence intensity or non-stationarity of the flow, while the position or Doppler shift (F) allows the determination of the mean advection velocity, given by $U_a = cF/[2v_0 \sin(\theta/2)]$. Like any flow property, U_a is independent of the scattering configuration. Following the same method utilized in a previous work [11], we conclude that the advection velocity is known with an error of 8.5%. For instance, when the angle θ goes to zero (forward scattering configuration), the vertical advection velocity becomes perpendicular to the incident wave vector $\vec{k}_i$ and $\vec{q} \rightarrow 0$ (see Fig. 1). This means that the Doppler shift F goes to zero in the expression for U_a, the ratio $F/\sin(\theta/2)$ remaining constant. If the scattered amplitude is measured in the forward direction ($\theta \sim 0°$), the signal is proportional to the time Fourier transform of the total vorticity of the flow. Measurement accuracy is limited by diffraction effects, which is estimated as the angular width of the diffraction lobe of transducers, being in this case around 3° at 40 kHz [8,9].

As detailed by Elicer-Cortés et al. [12], acoustic transducers are band-pass filters of response varying with the incoming ultrasound wave frequency v_0, with the distance between the transducers and with the scattering angle θ and the bias voltage of the transducers. Fig. 3 shows the

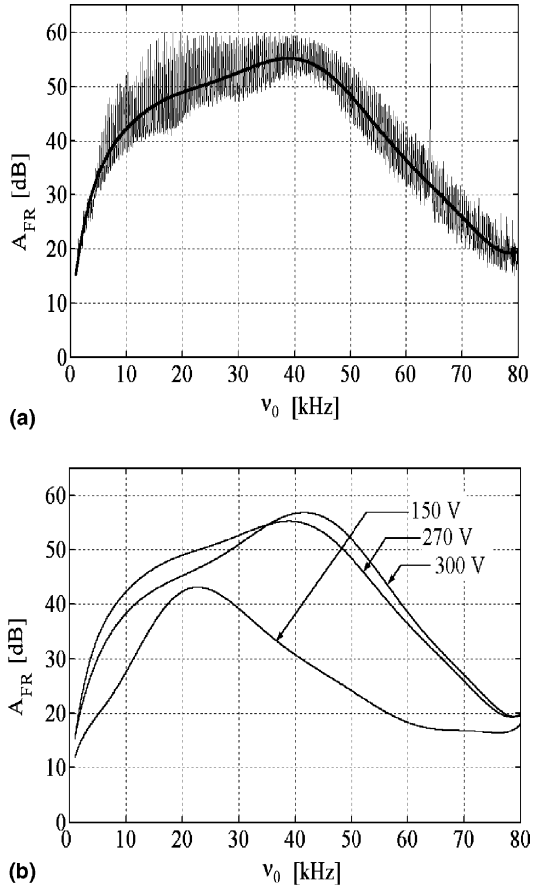

Fig. 3. Influence of the bias voltage on the response in ultrasound frequency of Sell transducers ($\theta = 50°$): (a) bias voltage 270 V; (b) bias voltage: 150 V, 270 V and 300 V.

frequency-dependent response of the transducers, A_{FR}, for a scattering angle of $\theta = 50°$. Transducers generally have a better response for frequencies in the range [10 kHz, 40 kHz]. The bias voltage was set to 270 V, a value that produced relatively small variations in the transducer response in that frequency range. To adjust for any variations in the transducer response, the normalized amplitude A_n (depending only on properties of the scattering medium) is obtained by dividing the measured scattered amplitude spectra A by A_{FR}:

$$A_n = \frac{A}{A_{FR}} = \frac{10^{\frac{A_{dB}}{20}}}{10^{\frac{A_{FR\,dB}}{20}}} \tag{3}$$

With the expressions in decibels defined as $A_{dB} = 10\log_{10}A^2$ and $A_{FR\,dB} = 10\log_{10}A_{FR}^2$. Following the same method utilized in a previous work [12], we find that the overall uncertainty in measuring A_n is 11.5%.

Both the transmitter and the receiver are acoustic transducers of the Sell type constructed as described in [23], of 15 cm in diameter, similar to those used in previous studies [8–14]. Baudet et al. [8] checked similar transducers using a calibrated BK4138 microphone, resulting amplitudes of the sound waves of the order of $P_0 \approx 1$ Pa. This pressure corresponds to a velocity associated to the incident wave of $|\vec{V}_{inc}| = (P_0/c\rho_0) \approx 0.24$ cm/s, much below the typical flow velocity, as required. A twin DC high voltage power supply (0–400 V) provided to both transducers a bias voltage. The acoustic emitter and receiver were mounted on traversing systems allowing vertical, horizontal and angular displacements. The set-up ensures an accurate determination of θ.

Previous studies have used ultrasound scattering to investigate turbulent or unsteady flows. Baudet et al. [8] considered a Von Kármán vortex street as a test flow and obtained spectral signals that agreed with the vortex shedding Strouhal frequency. Pinton et al. [9] studied a two-dimensional thermal plume, obtaining a spectrum characteristic of temperature fluctuations. Petrossian and Pinton [10] further considered a weakly heated turbulent air jet, verifying the existence of an inertial-convective subrange ($-5/3$ law). In previous experiments on axisymmetric turbulent thermal plumes, Elicer-Cortés et al. [11–14] verified theoretical predictions of Lund's works [21,22] and investigated the transition to turbulence and turbulence in development with respect to the distance to the heated source. The spatial anisotropy of the turbulent region was also investigated. In this paper, we present the first application of the ultrasound scattering technique to the study of mechanically excited thermal plumes. The study allowed the identification of preferred instabilities modes of flow (natural frequencies) and verifying the ability of thermal plumes to filter frequencies, acting as band-pass filters.

3. Experimental apparatus

The apparatus consisted of a thermal source immersed into quiescent air at atmospheric pressure inside a

$2.0 \times 2.0\ m^2$ square base, 2.5 m high, anechoic enclosure with double glazed walls. The anechoic properties of the enclosure were achieved after covering the inner walls with flexible polyurethane sheets of capacity of absorption over 90% for frequencies above 1 kHz, of density of 30 kg/m^3, of elasticity of up to 135% and of thermal conductivity of 0.25 W/(m K). An axisymmetric thermal plume was generated by an 8 mm thick round metallic disk of diameter $D = 80$ mm. The disk could be heated electrically up to 800 °C by a regulated AC power supply of 1 kV A. The heat release rate from the hot active surface of the disk ranged from 0 to 400 W. The temperature at the disk surface was measured with a thermocouple (K type) located 0.3 mm below the active surface. The lower part of the source was thermally insulated with 2.54 cm thick layers of rigid fiber. Holes in the lower part of the walls allowed the admission of fresh air. Holes were covered with synthetic fiber wool to avoid air blasts from the exterior. The enclosure was located in the basement of the laboratory to avoid significant fluctuations in the air temperature during the daytime and to reduce possible influence of external noises. Thus, the arrangement allowed the generation of almost ideal thermal plumes developing in an "infinite" adiabatic ambient fluid at rest. Air within the enclosure was not stratified [11,12].

The flow was mechanically excited by means of an oscillating toroidal metal ring of outer diameter 93 mm located at the periphery of the heat source, slightly downstream in order to disturb efficiently the plume entrainment. The position of the ring with respect to the hot disk was adjustable. Sinusoidal signals of a function generator TK-AFG-320 were applied to a speaker after amplification by a potential amplifier, model NF-HSA-4011. The periodic movement of the central part of a 15 cm diameter speaker was then transmitted to the ring by three thin rods 2 mm in diameter. The maximum amplitude of the movement of the ring was approximately 8 mm. To obtain axisymmetric disturbances, the ring axis was perfectly aligned with the source axis. The cross-section of the toroidal ring was only 5 mm in diameter in order to prevent the shedding of Von Kármán type vortices in the entrained airflow (of Reynolds number smaller than 50). Wake vortices were avoided in the vicinity of the source. A circular deflector was provided between the loudspeaker and the heat source to suppress any possible air pumping due to the movement of the loudspeaker.

Fig. 4 describes the experimental set-up and data recording. Ultrasound signals of sinusoidal shape and high frequency were generated by a HP-33120A function generator. The signals were amplified with a NF-4005 power amplifier and sent to the transmitter transducer that emitted a plane ultrasound wave of frequency v_0. The waves scattered from the measurement region were analyzed with the receiver transducer, that converted linearly the acoustic pressure into electric charges. The charges were sent to a BK-2635 charge amplifier, returning a voltage signal. This signal was received by a two-channel Lock-in amplifier SR-830. A narrow band frequency modulation eliminated all frequency components of the signal that are outside a frequency bandwidth $v_0 \pm \Delta v$. The eliminated frequencies did not contain any useful information. Here, Δv is the Doppler shift and the sign of Δv is determined from the relative position of the emitter and the receiver [11]. The output signal from the Lock-in amplifier was sampled and recorded on a Pentium PC mounted with an AT-A2150C acquisition board (16 bits AN converter and antialiasing filter). Signal processing and determination of vorticity spectra was achieved with Matlab programs. Other details on the experimental procedure can be found in recent papers [11–14].

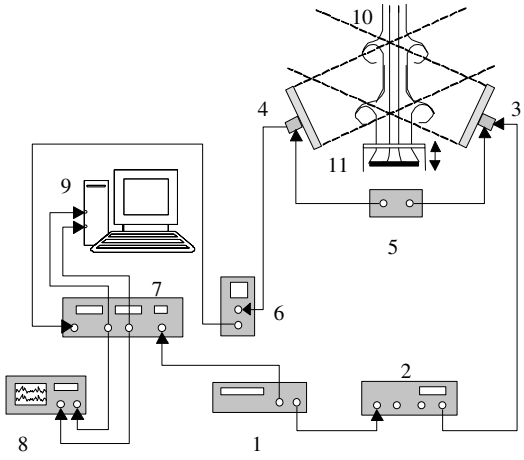

Fig. 4. Disposition of the instruments: (1) function generator; (2) power amplifier; (3) acoustic transmitter; (4) acoustic receiver; (5) twin DC power supply; (6) charge amplifier; (7) lock-in amplifier; (8) analog oscilloscope; (9) Pentium PC with acquisition board card; (10) thermal plume flow; (11) excitation apparatus.

4. Results and discussion

Source temperature varying between 100 °C and 200 °C was applied, a range where temperature fluctuations are low and vorticity can be considered as the only source of scattering. The scattering angle θ was set to 50°. Three temperatures were used, $T_d = 100$ °C, $T_d = 150$ °C and $T_d = 200$ °C, corresponding to global Grashof numbers (based on the disk diameter D) of $Gr = 3.22 \times 10^6$, $Gr = 3.84 \times 10^6$ and $Gr = 3.94 \times 10^6$, respectively. The unperturbed flows always remained laminar for these values, as shown by the Schlieren visualizations of Fig. 5 [24].

The frequency of the incoming sound wave varied between 5 kHz and 30 kHz, corresponding to length scales ranging from $l = 80$ mm to $l = 13$ mm ($l \approx c/[2v_0 \sin(\theta/2)]$). This choice is based on the fact that the primary vortical structures formed in the vicinity of the source have dimensions comparable to the source size ($D = 80$ mm in this case) [1,2,7]. The transducers were located near the heated disk to avoid interferences. The midpoint of the measurement volume (see Figs. 1 and 4) was 20 cm above the heated disk.

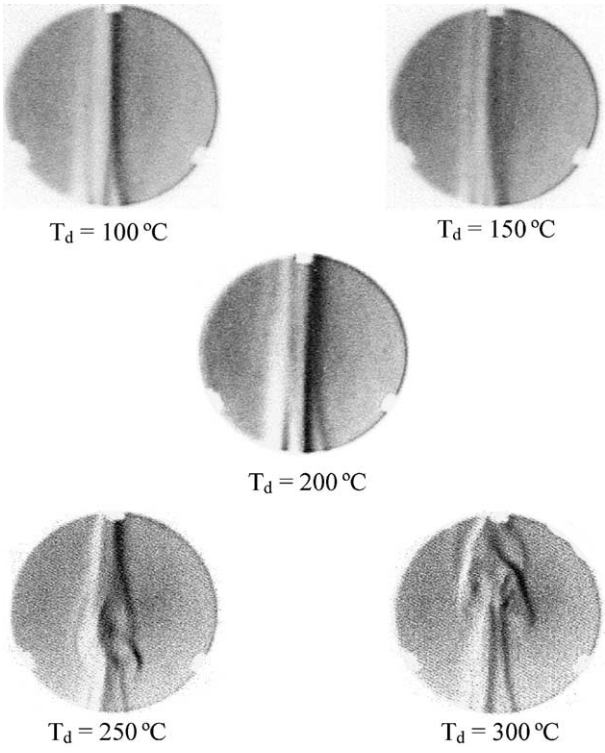

Fig. 5. Influence of the temperature on the stability of the thermal plume.

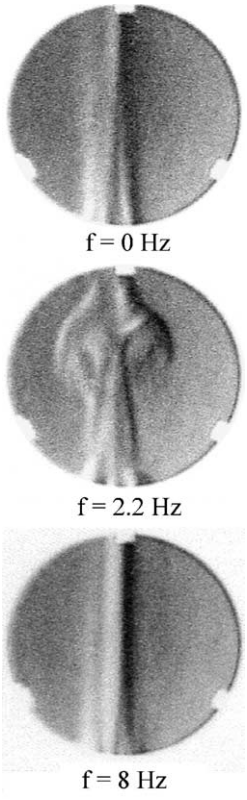

Fig. 6. Influence of the mechanical forcing frequency f on the stability of the laminar thermal plume: ($T_d = 150$ °C, $v_0 = 7.5$ kHz).

Fig. 2(a) shows a typical scattering signal [8–14], corresponding in this case to the response of an initially laminar thermal plume upon small mechanical excitations. The flow responds to imposed disturbances on entrainment by shedding vortical structures, as observed by Cetegen [7] in axisymmetric plumes of helium and air–helium mixtures. These data were obtained with a disk temperature of $T_d = 150$ °C and a frequency of the mechanical disturbance of $f = 2.5$ Hz (a frequency value corresponding to the largest flow response). The frequency of the incoming ultrasound wave was $v_0 = 7.5$ kHz, corresponding to a wavelength $l = 54$ mm. The advection velocity determined from the Doppler shift for this spectrum is close to $U_a = 30$ cm/s, in agreement with expected values and with the advection velocity $U_a = 28$ cm/s estimated from Schlieren visualizations [24]. In this latter case, the advection velocity of the vortical structures is given by considering the number of frames N necessary for a structure to cross the entire observation domain vertically (mirrors diameter, 6 in. or 0.15 m), the acquisition frame rate FR of the video camera being known ($U_a = 0.15$(FR/N) m/s). As shown in Fig. 2(b), when no disturbance is applied, the flow is laminar and does not exhibit any scattering peak; in agreement with the Schlieren visualizations of Fig. 6 (see also [24]). Note that in the absence of scattering, the acoustic signal is very weak. A depletion below the noise level (in dB scale) around v_0 is even observed. This depletion is due to the way the incident wave is removed electronically by the SR-830 Lock-in amplifier from the signal received by the receiver transducer.

When the incoming ultrasound wave frequency (i.e., the characteristic size of the structure under observation) is changed, keeping the same values ($T_d = 150$ °C, $f = 2.5$ Hz), a similar behavior is observed: an absence of scattering peak in the unperturbed systems, a peak when the perturbation is applied. The shape of the scattering peak depends on the ultrasound frequency. As shown in Fig. 7, the magnitude of the scattering peak decreases as the incoming ultrasound frequency increases, taking the values 7.5 kHz, 12.5 kHz and 17.5 kHz (i.e., structure size of 54 mm, 32 mm and 23 mm, respectively). It is interpreted by the fact that the vorticity modulus of small vortical structures is smaller. On the other hand, the scattering spectrum broadens as the ultrasound frequency increases, indicating that the advection velocity of small structures suffers larger fluctuations.

Fig. 8 illustrates the typical evolution of the scattering signal as the mechanical forcing frequency is increased. (Similar behavior was observed for all ultrasound frequencies used in this study). The plots of Fig. 8 were obtained for $T_d = 150$ °C and $v_0 = 12.5$ kHz. At mechanical forcing frequencies around $f = 1$ Hz, no scattering is detected. The flow remains stable in a range of low mechanical forcing frequencies. The absence of vortices was independently verified by means of Schlieren visualization [24]. The fact that no scattering signal appears in this regime provides an indirect verification that temperature inhomogeneities are too weak to scatter the ultrasound wave. Otherwise, a

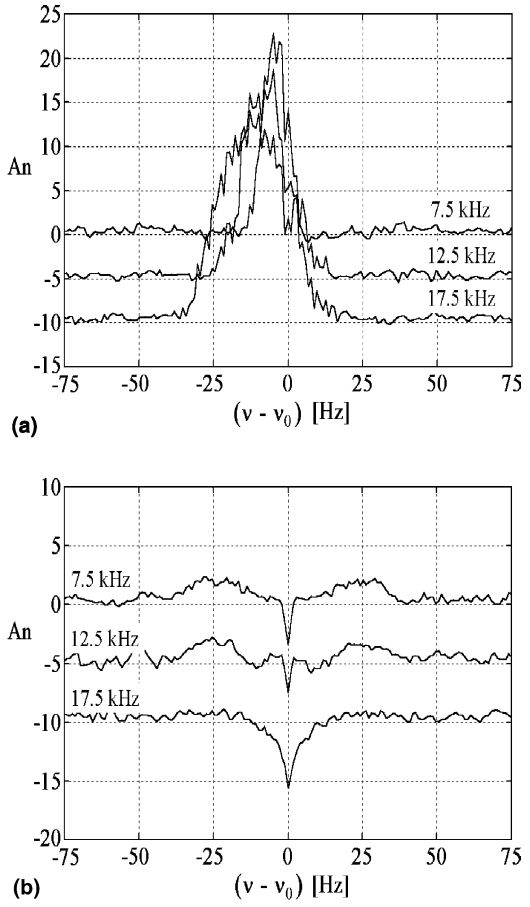

Fig. 7. Normalized amplitude of the scattering peak—influence of the ultrasound frequency ($T_d = 150\,°C$, $\nu_0 = 7.5$ kHz): (a) for disturbed condition, ($f = 2.5$ Hz); (b) for no disturbed condition, ($f = 0.0$ Hz).

scattering peak, even small, would be observed. The scattering peak reaches its highest value around a forcing frequency $f = 2$ Hz. As the forcing frequency further increases, the magnitude of the peak decreases. The vorticity generated by mechanical forcing therefore becomes weaker as f increases away from the resonance, or maximal flow response. When the forcing frequency is larger than $f = 6$ Hz, the scattering signal is practically at the noise level, indicating a relaminarization of the flow. The resonance around $f = 2$ Hz seems to correspond to a natural mode of the plume. This value falls within the interval of natural frequencies associated to temperature fluctuations found by Brahimi [25] with cold wire thermometry (for round thermal plumes of $Gr = 2.7 \times 10^7$) in the Boussinesq zone of the flow. This interval of thermal natural frequencies is comprised between 1.5 Hz and 2.5 Hz. In our experiments the heating is relatively low, the Boussinesq's hypothesis holds (the Prandtl number is about 0.7), and our results can be compared with Brahimi's.

The ultrasound spectra of Fig. 8 obtained for $f = 2$ Hz and $f = 4$ Hz are fairly regular. On the other hand, at $f = 3$ Hz, $f = 5$ Hz and $f = 6$ Hz, irregularities characterized by saw teeth profiles superpose to the main scattering peak, leading to multiple peaks. These peaks are shifted away from ν_0 by an amount equal to the forcing frequency and its harmonics. The emergence of these secondary peaks (irregularities) is attributed to oscillations of the mean downstream flow. In the spectrum at $f = 3$ Hz, the peaks are enveloped by a wider bell-curve along the ν-axis. Moreover, the spectra at higher forcing frequency ($f = 5$ Hz and 6 Hz) are characterized by multiple peaks with sharp variations; only irregularities appear and the scattering peak revealing vortical structures is lost. In contrast, Schlieren visualizations [24] indicate the presence of a wave traveling at the forcing frequency through the laminar flow. These small undulations do not destabilize the plume. The ultrasound flow detection technique detects these undulations that do not produce ultrasound scattering, appearing in the spectra showing peaks to the forcing frequency and its harmonics.

Fig. 9 shows the normalized amplitude of scattering peak, A_n, as a function of the incoming sound wave frequency (inferior abscissa), or, equivalently, as a function of the wavelength (superior abscissa). The three separate figures correspond to three different source temperatures. Each plotted curve is obtained for a particular forcing frequency. Each point is determined by arithmetic average of five runs of 30-s integration of the scattered pressure.

To any given probe ultrasound frequency ν_0 corresponds a wave number $|\vec{q}|$ in the Fourier space for the vorticity (see Eq. (1)). The fact that the Fourier spectrum is relatively broad indicates that the vortex generated mechanically is spatially localized, which is to be expected. The data are also time averaged and each frequency spectra corresponds to the passage of various vortices, that can be fluctuating in shape.

The shape of the curves of Fig. 9 has two "hills" (denoted as first and second maximum) separated by one "valley". The first maximum is located in a range of incoming ultrasound frequencies of $\nu_0 = 5$ kHz to $\nu_0 = 7.5$ kHz, or scanned structures of sizes between $l = 80$ mm and $l = 54$ mm. These large structures are of order of the source diameter, in agreement with the size of the structures observed by Cetegen [2] close to the heated source. When advected downstream they cause a turbulent state in the flow. The second maximum is located between $\nu_0 = 20$ kHz and $\nu_0 = 25$ kHz, corresponding to smaller structures, of sizes ranging from $l = 20$ mm to $l = 16$ mm. Note that for a fixed mechanical forcing frequency roughly equal or larger than $f = 5$ Hz, the magnitude of the scattered signal increases with the ultrasound frequency in the higher frequency range ($\nu_0 > 20$ kHz). This indicates the presence of relatively small structures with important levels of vorticity. The size of these structures is around $l = 14$ mm, and their vorticity is comparable to that of the second maximum. Again, these results agree with the findings of Cetegen [2], who observed small scale instabilities in the region near the mechanical forcing. These preferential instability modes can be attributed to natural resonant frequencies of a flow.

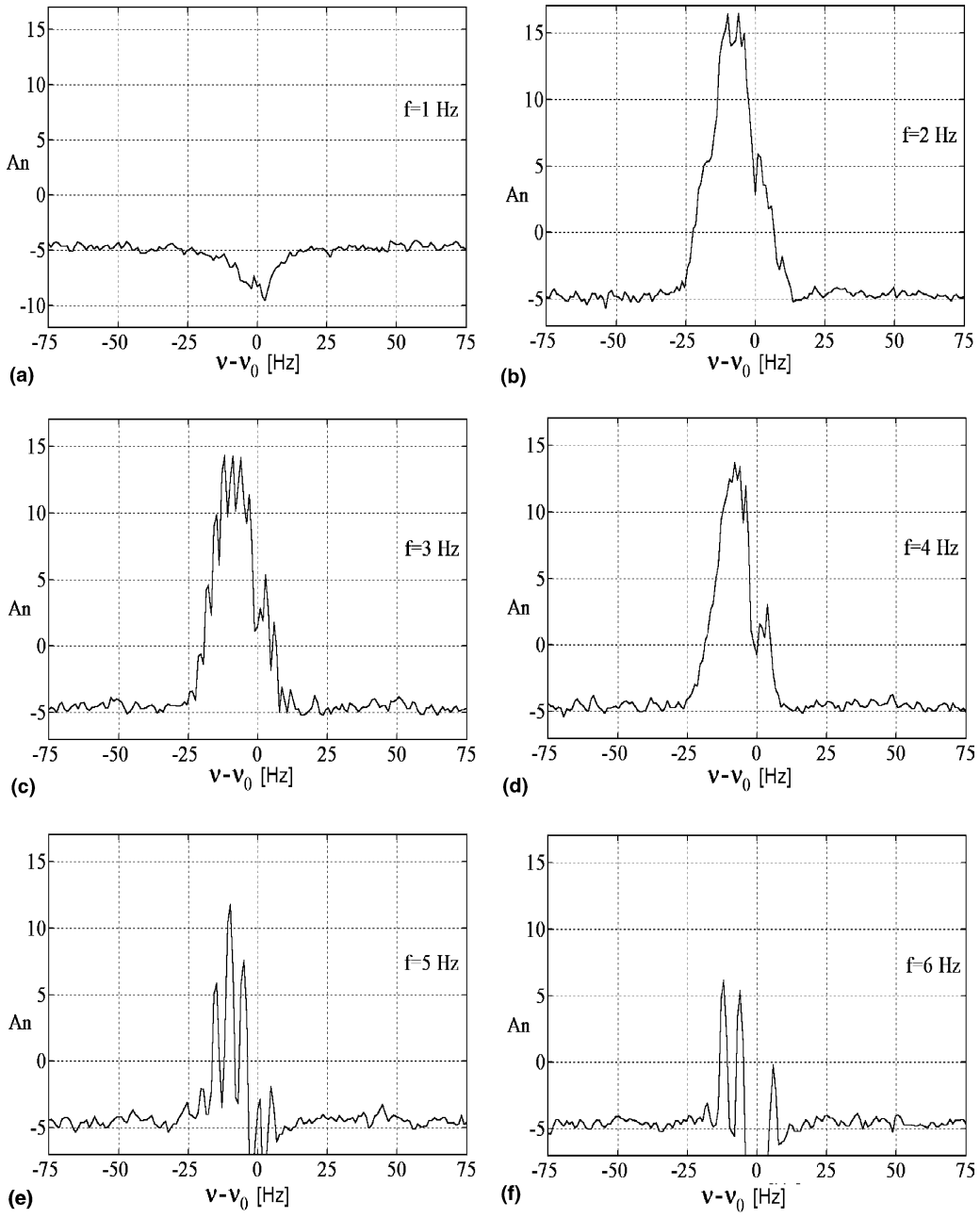

Fig. 8. Normalized amplitude of the scattering peak—influence of the mechanical forcing frequency, ($T_d = 150\,°C$, $v_0 = 12.5\,kHz$): (a) $f = 1$ Hz; (b) $f = 2$ Hz; (c) $f = 3$ Hz; (d) $f = 4$ Hz; (e) $f = 5$ Hz; (f) $f = 6$ Hz.

The "valley" region of relatively low scattering intensity lies in the ultrasound frequency range [15 kHz, 17.5 kHz], or wavelengths between $l = 27$ mm and 23 mm. The three plots of Fig. 9 show that the depth of the valley increases as the temperature of the heated source increases. In addition, the surrounding peaks become narrower. In terms of vortex formation, it means that the length scales associated to the vortical structures are more sharply defined as the temperature increases. In other words, depending on the temperature (or Grashof number), the range of possible sizes of preferential instabilities can be made more or less narrow.

Fig. 9 indicates that the magnitude of the vorticity of the instabilities depends on the frequency of the mechanical disturbance. Fig. 10 displays the maximum value of the first "hill" as a function of the forcing frequency, for different temperatures. For disturbance frequencies close to $f = 1$ Hz, no scattering peak can be detected with the precision given by the apparatus. Increasing the disturbance frequency between $f = 1$ Hz and $f = 2$ Hz leads to an important increase of the amplitude of the scattering peak. The laminar flow loses stability and the shedding of vortical structures predominates. After the maximum amplitude value around $f = 2$ Hz, the vorticity decays gradually down to low values. Mechanical disturbances of the plume induce vortex formation within a finite frequency range. For the source temperatures used, this range is roughly located

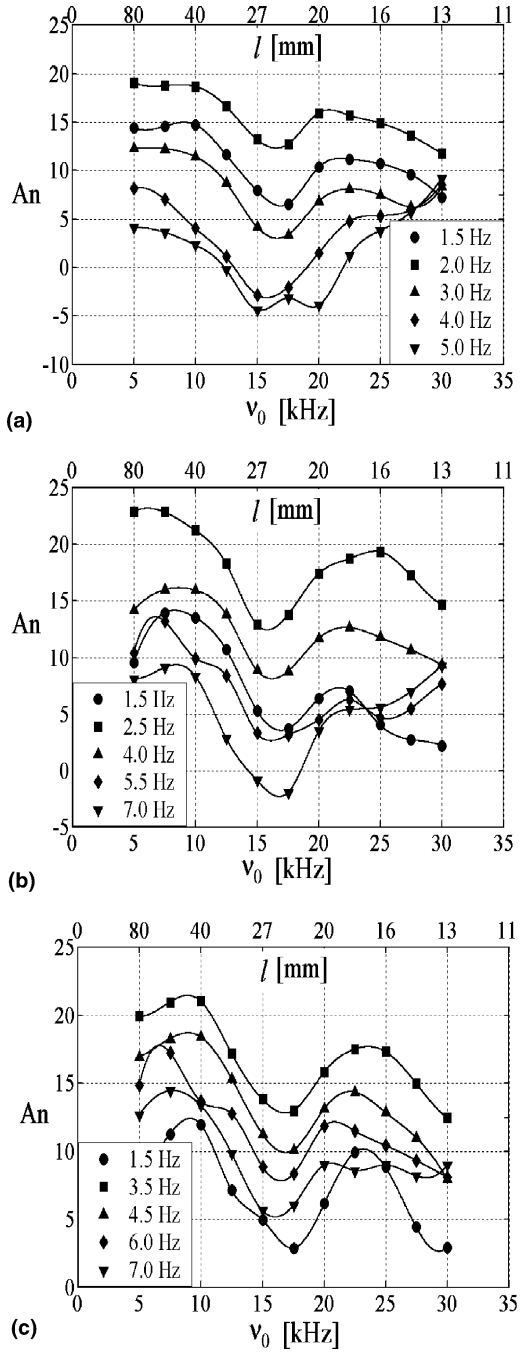

Fig. 9. Evolution of the normalized amplitude of the scattering peak with the incoming ultrasound wave frequency—influence of the mechanical forcing frequency and temperature: (a) $T_d = 100\ °C$; (b) $T_d = 150\ °C$; (c) $T_d = 200\ °C$.

between $f = 1$ Hz and $f = 10$ Hz, in agreement with the stability analysis carried out by Pera and Gebhart [4]. Mechanical disturbance of high frequency do not alter the stability of plume. It seems that thermal plume have a filtering ability, in agreement with observations reported by Bill and Gebhart [5] and Kimura and Bejan [6].

Making an analogy between the three curves of Fig. 10 and band-pass filters, we conclude that the bandwidth where disturbances are amplified increases as the temperature of the heated source increases. For $T_d = 100\ °C$ the plume responds for frequencies between $f = 1$ Hz and $f = 5$ Hz. For $T_d = 150\ °C$ and $T_d = 200\ °C$ it responds for frequencies ranging from $f = 1$ Hz and $f = 7$ Hz. In Fig. 10, the slope of curves after the resonance (indicating how the vorticity decays with f) become less pronounced as the source temperature is increased. In addition, at higher temperatures, the mechanical resonance is slightly shifted toward higher forcing frequency values. For $T_d = 100\ °C$, the maximum is located around $f = 2$ Hz; for $T_d = 150\ °C$, near $f = 2.5$ Hz; and for $T_d = 200\ °C$, near$f = 3$ Hz.

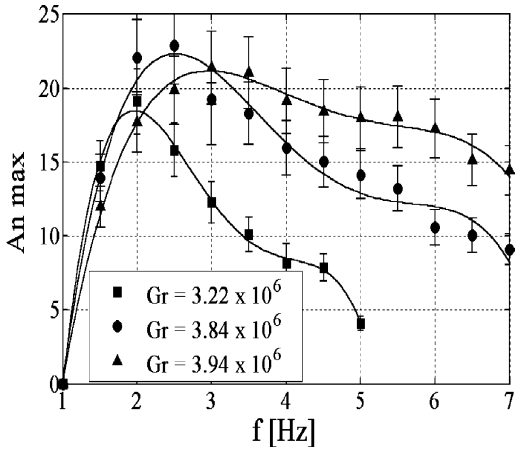

Fig. 10. Maxima of the normalized amplitude of the scattering peak versus the mechanical forcing frequency—influence of the Grashof number.

5. Conclusions

A measurement technique based on ultrasound scattering by vorticity was used to characterize instabilities in an initially laminar, axisymmetric thermal plume subjected to controlled symmetric disturbances. Thermal plumes responded to external symmetric disturbances of varicose mode (imposed on entrainment) by shedding vortical structures. These structures were analyzed with the ultrasound spectra. Temperature inhomogeneities barely contributed to scattering.

Particular flow length scales were studied by tuning the ultrasound frequency accordingly. It is known from earlier experiments [1,2,7] that the primary vortical structures are formed close to heated source and have dimensions comparable to the source size.

In the absence of any disturbance, the flow remained laminar and stable for the source temperatures imposed. No scattered ultrasound waves were detected in that regime, and the absence of vortices was corroborated with Schlieren visualizations [24].

When the mechanical disturbance was applied, a peak appeared in the scattering signal. By changing the incoming ultrasound frequency, i.e., the size of structures under observation, the shape of the scattering peak was slightly

modified. Its height exhibited relatively changes, indicating variations of vorticity. On the other hand, the scattering peak become wider as the structure size decreased, indicating that the advection velocity of small vortices had larger fluctuations around the mean flow.

The evolution of scattering peak with respect to the mechanical forcing frequency shows that the flow does not respond to low frequencies: it remains laminar for frequencies lower than $f = 1$ Hz. This observation was verified by Schlieren visualization. The scattering signal is maximum at a mechanical forcing frequency around $f = 2$ Hz. Further increase in f produces a decrease in the vorticity (that eventually vanishes), and therefore weaker sound/flow interactions. The flow relaminarizes at high frequencies, as also observed by the Schlieren technique.

The normalized amplitude of the scattering peak, A_n, shows two maxima when plotted as a function of the ultrasound probe frequency. The first region of wavelengths of preferred instabilities ranges from $l = 80$ mm to $l = 54$ mm, lengths of order of the heated source diameter, a finding in agreement with previous studies [2]. The second region ranges from $l = 20$ mm to $l = 16$ mm. These preferential spatial modes are attributed to modes or natural frequencies of the flow. As the temperature is increased, the region of relatively low scattering intensity separating both maxima becomes deeper and the width of the maxima becomes narrower. Therefore, the length scales of the vortices generated mechanically become more sharply defined around two typical values when the source temperature is increased. The vorticity of these preferential modes depends on the frequency of the mechanical disturbance. The vorticity reaches a maximum (resonance) value for a disturbance frequency close to $f = 2$ Hz, corresponding to a natural frequency of flow. The resonance frequency increases as the temperature is increased. After the resonance, vorticity decays gradually with the forcing frequency. Disturbances of high frequency do not alter the stability of plume, in agreement with findings of other studies [5,6]. Thermal plumes seem to have a filtering ability, and act as band-pass filters. As the temperature of the heated source increases, the bandwidth where a plume is able to amplify disturbances becomes larger.

Acknowledgment

The study reported in this paper was supported by CONICYT under grant FONDECYT No 1010135 and 7010135. We gratefully acknowledge the valuable scientific, technical and material support of Dr. Christophe Baudet.

References

[1] B.M. Cetegen, Y. Dong, M.C. Soteriou, Experiments on stability and oscillatory behavior of planar buoyant plumes, Phys. Fluids 10 (7) (1998) 1658–1665.

[2] B.M. Cetegen, A phenomenological model of near-field fire entrainment, Fire Safety J. 31 (1998) 299–312.

[3] B. Gebhart, Y. Jaluria, R. Mahajan, B. Sammakia, Buoyancy-Induced Flows and Transport, Textbook Edition., Hemisphere Publishing Corporation, 1988.

[4] L. Pera, B. Gebhart, On stability of laminar plumes: some numerical solution and experiments, Int. J. Heat Mass Transfer 14 (1971) 975–984.

[5] R.G. Bill, B. Gebhart, The transition of plane plumes, Int. J. Heat Mass Transfer 18 (1975) 513–526.

[6] S. Kimura, A. Bejan, Mechanism for transition to turbulence in buoyant plumes flow, Int. J. Heat Mass Transfer 26 (1983) 1515–1532.

[7] B.M. Cetegen, Behavior of naturally unstable and periodically forced axisymetric buoyant plumes of helium and helium–air mixtures, Phys. Fluids 9 (12) (1997) 3742–3757.

[8] C. Baudet, S. Ciliberto, J.F. Pinton, Spectral analisys of the Von Kárman flow using ultrasound scattering, Phys. Rev. Lett. 67 (1) (1991) 193–195.

[9] J.F. Pinton, C. Laroche, S. Fauve, C. Baudet, Ultrasound scattering by buoyancy driven flow, J. Phys. II France 3 (1993) 767–773.

[10] A. Petrossian, J.F. Pinton, Sound scattering on a turbulent, weakly heated jet, Physique II France 7 (1997) 801–812.

[11] J.C. Elicer-Cortés, C. Baudet, Ultrasound scattering from a turbulent round thermal pure plume, Exp. Therm. Fluid Sci. 18 (1999) 271–281.

[12] J.C. Elicer-Cortés, J. Fuentes, A. Valencia, C. Baudet, Experimental study of transition to turbulence of a round thermal plume by ultrasound scattering, Exp. Therm. Fluid Sci. 20 (2000) 137–149.

[13] J.C. Elicer-Cortés, R. Contreras, D. Boyer, M. Pavageau, R.H. Hernández, Temperature spectra from a turbulent thermal plume by ultrasound scattering, Exp. Therm. Fluid Sci. 28 (2004) 803–813.

[14] J.C. Elicer-Cortés, J. Tapia, M. Pavageau, Detection and estimation of the isotropy degree of temperature scales in a turbulent thermal plume by ultrasound scattering, Int. Commun. Heat Mass Transfer 30 (7) (2003) 931–944.

[15] A.M. Obukhov, Über die schallstreuung in der turbulenten strömung, Dokl. Akad. Nauk. SSSR 30 (1941) 616–620.

[16] M.J. Lighthill, On sound generated aerodynamically I, general theory, Proc. R. Soc. A 211 (1952) 564–587.

[17] R.H. Kraichnan, The scattering of sound in a turbulent medium, J. Acoust. Soc. Am. 25 (6) (1953) 1096–1104.

[18] B.T. Chu, L.S.G. Kovásznay, Nonlinear interactions in a viscous heat-conducting compressible gas, J. Fluid Mech. 3 (5) (1958) 494–514.

[19] V.Y. Tatarskii, Wave Propagation in a Turbulent Medium, McGraw-Hill, New York, 1961.

[20] W. Baerg, W.H. Schwarz, Measurements of the scattering of sound from turbulence, J. Acoust. Soc. Am. 39 (6) (1966) 1125–1132.

[21] F. Lund, C. Rojas, Ultrasound as a probe of turbulence, Physica D 37 (1989) 508–514.

[22] H. Contreras, F. Lund, Ultrasound as a probe of turbulence II. Temperature inhomogeneities, Phys. Rev. Lett. A 149 (1990) 127–130.

[23] D. Anke, Luftschallwandler nach dem Sell-Prinzip für Frequenzen von 50 kHz bis 100 kHz, Acustica 30 (1974) 30–39.

[24] J.C. Elicer-Cortés, C. Ruz, R.H. Hernández, M. Pavageau, D. Boyer, Observation of preferred instability modes in a mechanically excited thermal plume using Schlieren visualization, Int. Commun. Heat Mass Transfer 32 (2005) 360–370.

[25] M. Brahimi, Structure turbulente des panaches thermiques—Interaction, Thèse de Docteur d'Université, Université de Poitiers, France, 1987.